Regulation of the mitochondrial dynamin-like protein Opa1 by proteolytic cleavage

Lorena Griparic, Takayuki Kanazawa, and Alexander M. van der Bliek

Department of Biological Chemistry, David Geffen School of Medicine, University of California, Los Angeles, Los Angeles, CA 90095

The dynamin-related protein Opa1 is localized to the mitochondrial intermembrane space, where it facilitates fusion between mitochondria. Apoptosis causes Opa1 release into the cytosol and causes mitochondria to fragment. Loss of mitochondrial membrane potential also causes mitochondrial fragmentation but not Opa1 release into the cytosol. Both conditions induce the proteolytic cleavage of Opa1, suggesting that mitochondrial fragmentation is triggered by Opa1 inactivation. The opposite effect was observed with knockdown of the mitochondrial intermembrane space protease Yme1. Knockdown of Yme1 prevents the constitutive cleavage of a subset of Opa1 splice variants but does not affect carbonyl cyanide *m*-chlorophenyl hydrazone or apoptosis-induced cleavage. Knockdown of Yme1 also increases mitochondrial connectivity, but this effect is independent of Opa1 because it also occurs in Opa1 knockdown cells. We conclude that Yme1 constitutively regulates a subset of Opa1 isoforms and an unknown mitochondrial morphology protein, whereas the loss of membrane potential induces the further proteolysis of Opa1.

Introduction

Dominant optic atrophy is a progressive eye disease resulting from degeneration of the retinal ganglion cell layer with ascending atrophy of the optic nerve. The disease is most often caused by mutations in the OPA1 gene, which encodes a human homologue of yeast Mgm1 (Votruba, 2004). Mgm1 and Opa1 are members of the dynamin family of GTP-binding proteins (van der Bliek, 1999). The mitochondria of yeast Mgm1 mutants are fragmented because of a defect in mitochondrial fusion (Meeusen and Nunnari, 2005; Meeusen et al., 2006). Transfection of mammalian cells with Opa1 siRNA or with dominant interfering constructs also causes mitochondria to fragment. In addition, the loss of Opa1 causes cell death, suggesting an antiapoptotic function that may contribute to dominant optic atrophy (Olichon et al., 2003; Griparic et al., 2004; Arnoult et al., 2005).

Yeast Mgm1 and mammalian Opa1 have N-terminal mitochondrial targeting signals that are cleaved by the mitochondrial matrix processing protease. Yeast Mgm1 and mammalian Opa1 reside in the mitochondrial intermembrane space, where they are tightly bound to or embedded in the inner membrane (Wong et al., 2003). A substantial fraction of yeast Mgm1 is further processed by a rhomboid protease called Pcp1, which is required

for normal Mgm1 function (van der Bliek and Koehler, 2003). Yeast Pcp1 mutants can be rescued by the heterologous expression of a mammalian Pcp1 homologue called presenilin-associated rhomboid-like (PARL; McQuibban et al., 2003). However, only 4% of Opa1 is processed by PARL (Cipolat et al., 2006; Frezza et al., 2006), whereas a much larger fraction of Opa1 is cleaved by a protease that is induced with the loss of mitochondrial membrane potential or apoptosis (Duvezin-Caubet et al., 2006; Ishihara et al., 2006). Moreover, PARL knockout cells have normal mitochondrial morphologies (Cipolat et al., 2006), whereas cells with an induced proteolysis of Opa1 have fragmented mitochondria (Duvezin-Caubet et al., 2006), suggesting different roles for PARL in mammals and yeast.

Experiments with the heterologous expression of mammalian Opa1 in yeast suggest that a mitochondrial matrix protease called paraplegin can process Opa1, but paraplegin siRNA has only modest effects on Opa1 in mammalian cells (Ishihara et al., 2006). The N terminus of mammalian Opa1 also undergoes extensive alternative slicing near the point of cleavage (Satoh et al., 2003). Cleavage could conceivably affect the attachment of Opa1 to the membrane because Opa1 is released from mitochondria coincident with the cleavage that occurs during apoptosis (Arnoult et al., 2005). The mechanism of release and its functional consequences are not yet known.

In this study, we confirm the release of Opa1 during apoptosis and show that this coincides with the proteolytic cleavage

of Opa1. Transfection with PARL siRNA and PARL knockout did not affect Opa1 maturation nor did it affect induced proteolysis, suggesting that other proteases are responsible for these cleavages. Investigation of known mitochondrial proteases by transfection with siRNA shows that the mitochondrial intermembrane space protease Yme1 affects the constitutive processing of Opa1. Yme1 also affects mitochondrial morphology, but this property is independent of Opa1.

Results and discussion

Inducible proteolysis and release of Opa1

Mature Opa1 can be resolved into five bands ranging in size from 85 to 100 kD on Western blots (Fig. 1 A). The bands, which are named a through e, correspond to different isoforms (Olichon et al., 2007). Treatment with apoptosis-inducing agents causes the larger isoforms to disappear from mitochondrial fractions, whereas shorter isoforms appear in the cytosol (unpublished data). This shift is not affected by cycloheximide, indicating that Opa1 undergoes inducible proteolysis and release from mitochondria rather than altered protein synthesis. Release of Opa1 occurs in the presence of the caspase inhibitor zVAD-fmk like release of cytochrome c but unlike that of apoptosis-inducing factor, which is inhibited by zVAD-fmk (Table S1, available at http://www.jcb.org/cgi/content/full/jcb.200704112/DC1). Opa1 proteolysis also occurs within 12 min after adding carbonyl cyanide m-chlorophenyl hydrazone (CCCP), which induces the loss of mitochondrial membrane potential. The mitochondria of CCCP-treated cells convert to an abundance of tiny fragments similar to the fragmentation that occurs during apoptosis (Fig. 1 B). However, CCCP does not cause the release of Opa1 or cytochrome c into the cytosol nor does it trigger apoptosis even after 5.5 h of incubation, as shown by the lack of caspase 9 cleavage (Fig. 1 A). CCCP-induced cleavage is also not enough to release Opa1 from the inner membrane because a substantial fraction of the cleaved protein remains membrane bound, as determined with carbonate extraction (unpublished data). Removal of CCCP allows for the gradual recovery of wild-type mitochondrial morphology and of the larger Opa1 isoforms (Fig. S1). This recovery is blocked by cycloheximide, showing that it requires the de novo synthesis of Opa1.

siRNA of mitochondrial proteases

To find out which proteases affect Opa1, we conducted knockdown experiments with siRNA directed against known mitochondrial
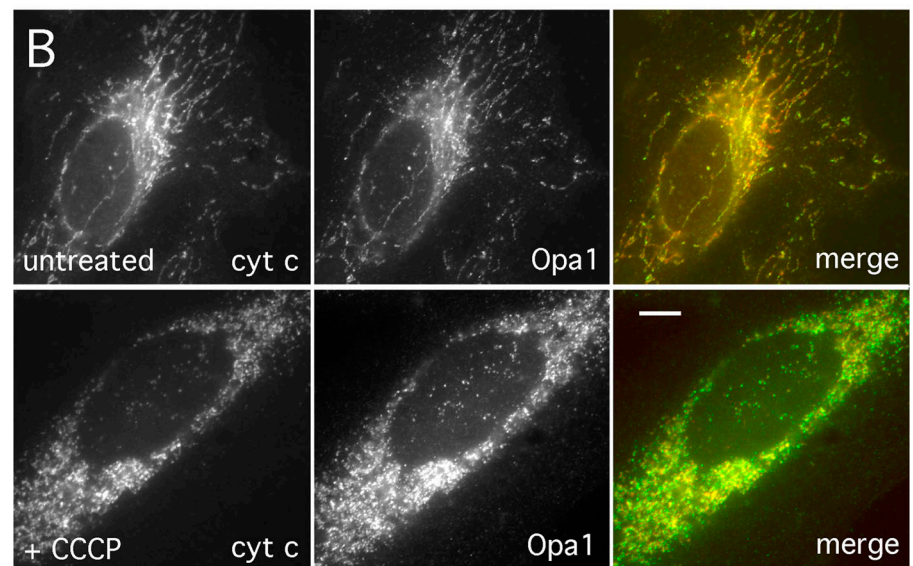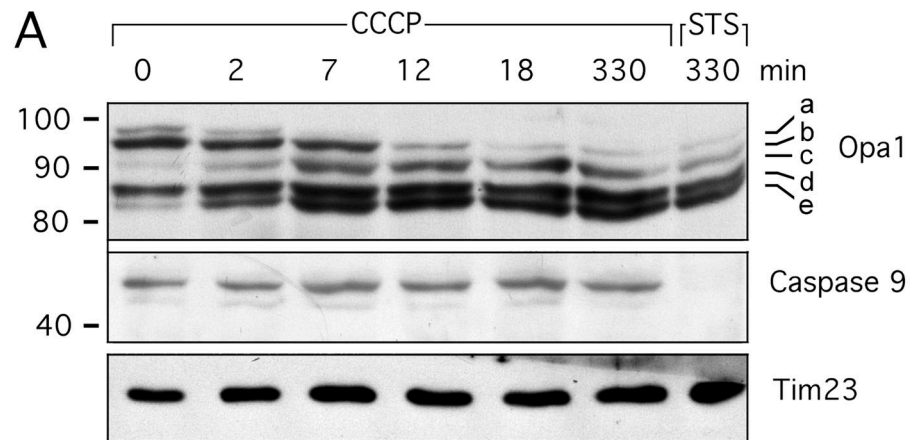

Figure 1. **The loss of mitochondrial membrane potential is enough to induce Opa1 proteolysis.** (A) Western blots of cells treated for increasing lengths of time with CCCP show a shift in Opa1 isoforms. Tim23 serves as a loading control. Lack of cleavage of caspase 9 shows that CCCP did not induce apoptosis. Staurosporine (STS)-induced cleavage serves as a positive control. Opa1 bands were labeled a, b, c, d, and e as previously described (Duvezin-Caubet et al., 2006; Ishihara et al., 2006; Olichon et al., 2007). (B) A 5.5-h incubation with CCCP causes mitochondria to fragment but does not cause the release of cytochrome c or Opa1 into the cytosol. The merged images show cytochrome c in red and Opa1 in green. Bar, 10 μm.

proteases. The rhomboid protease PARL was considered a likely candidate because it is very similar to yeast Pcp1. PARL siRNA was highly effective (Fig. 2 A). However, transfection with PARL siRNA had no effect on Opa1 maturation or inducible proteolysis. Because a small amount of residual PARL could still account for inducible cleavage, we also tested a PARL knockout mouse embryonic fibroblast cell line (Cipolat et al., 2006). We find that PARL$^{-/-}$ cells already show a substantial amount of Opa1 proteolysis even without CCCP. This cleavage may reflect the increased susceptibility to apoptosis that was previously observed with PARL$^{-/-}$ mice (Cipolat et al., 2006) and by us with PARL siRNA (unpublished data). However, this

cell line is still capable of inducible cleavage (Fig. 2 C). The existence of inducible cleavage in these cells was confirmed by transfection with selected Opa1 isoforms and treatment with CCCP. Overexpression of Opa1 isoform 7 in PARL knockout cells showed some changes in the intensities of bands c and d (Fig. 2 C, bottom), but these intensities varied between experiments, suggesting that PARL is not required for constitutive cleavage nor is it required for inducible cleavage.

Another candidate is HtrA2/Omi, which faces the mitochondrial intermembrane space (Seong et al., 2004). HtrA2/Omi siRNA was highly effective (>99.4% reduction as judged by densitometry of the Western blot), but this did not noticeably

Figure 2. **Effects of known mitochondrial proteases on Opa1 proteolysis.** (A) Cells were transfected with siRNA for the different proteases. Scrambled oligonucleotides served as controls. PARL was reduced by 92%, Yme1 was reduced by 72%, and HtrA2/Omi was reduced by 99.4% on Western blots. Proteolysis was induced with CCCP (60 min). DMSO (solvent) served as a control. For Yme1 and PARL siRNA, proteolysis was also induced with staurosporine (3 h). Data are representative of three independent experiments. (B) Densitometry of Opa1 bands in Yme1 siRNA–transfected cells with or without CCCP. The histogram shows the relative intensity of bands. (C) PARL$^{-/-}$ cells show enhanced degradation but still possess the inducible cleavage of Opa1. Endogenous protein was detected with Opa1 antibody. Transfected isoforms were detected with a C-terminal myc tag. The two cleavage products of isoform 7 correspond to cleavage in exon 5 (S1) and exon 5b (S2). (D) Effects of Yme1 siRNA on isoform 1, 5, and 7 cleavage with or without CCCP induction and deletion of the S1 cleavage site. (E) Densitometry of the uninduced lanes (DMSO) in D. A plus symbol after Delta S1 indicates an S1 cleavage site deletion (Ishihara et al., 2006). A plus symbol after Yme1 indicates transfection with Yme1 siRNA.

affect Opa1 proteolysis (Fig. 2 A). Lastly, we tested mitochondrial AAA proteases. Mammals have three of these, namely Yme1, paraplegin, and AFG3L2 (Langer et al., 2001). The catalytic domain of Yme1 faces the mitochondrial intermembrane space, whereas those of paraplegin and AFG3L2 face the mitochondrial matrix. Transfection with paraplegin and AFG3L2 siRNA did not affect Opa1 proteolysis, but knockdown was incomplete (10 and 34% residual RNA), so paraplegin or AFG3L2 might still mediate inducible cleavage.

In contrast, Yme1 siRNA did affect Opa1 even without CCCP. Western blots show shifts in banding patterns in treated and untreated cells (Fig. 2 A). CCCP still induces proteolysis in Yme1 siRNA–transfected cells, whereas not all bands are equally affected by Yme1 siRNA and CCCP (Fig. 2 B), suggesting that the cleavage patterns are governed by alternative splicing. We conclude that Yme1 affects the constitutive proteolysis of a subset of Opa1 isoforms but is not required for inducible proteolysis.

Opa1 has extensive alternative splicing near the sites of cleavage (Ishihara et al., 2006). To determine which splice variants are affected by inducible proteolysis and which are affected by Yme1-mediated proteolysis, we transfected cells with representative expression constructs (isoform 1 has no extra exon, isoform 5 has 4b but not 5b, and isoform 7 has 5b but not 4b; Satoh et al., 2003). All three isoforms are relatively abundant in HeLa cells (Satoh et al., 2003; Olichon et al., 2007). In addition, we transfected cells with expression constructs in which the major inducible cleavage site S1, which is contained by exon 5, was deleted (Ishihara et al., 2006). The transfected cells were treated with or without CCCP to determine their sensitivity to inducible proteolysis and were cotransfected with or without Yme1 siRNA to determine their sensitivity to constitutive proteolysis.

Our results confirm that isoform 1 is cleaved by CCCP-inducible proteolysis (Fig. 2, D and E). Mutations in S1, the cleavage site that was previously shown to exist in exon 5, render this isoform insensitive to inducible cleavage (Ishihara et al., 2006). However, this isoform is not affected by Yme1 siRNA. In contrast, isoform 5 and isoform 7, which contain exon 4b and exon 5b, respectively, are affected by Yme1 siRNA. In both cases, there is a substantial shift to the uncleaved band. Residual cleavage to the lower bands in uninduced cells and further cleavage upon induction with CCCP can be attributed to the inducible protease.

Isoform 5, which contains exon 4b, is fully cleaved even without CCCP induction (Fig. 2, D and E). This cleavage is reduced but not fully eliminated by deleting S1, and it is reduced but not fully eliminated by transfection with Yme1 siRNA. However, the uncleaved protein that accumulates under these conditions can be cleaved by inducible proteolysis even when S1 is deleted. We conclude that isoform 5 has an alternative cleavage site similar to the alternative cleavage site in isoform 7. Sizing by SDS-PAGE suggests that this site is in exon 4b (unpublished data), which is analogous to the alternative cleavage site S2 in exon 5b of isoform 7.

Isoform 7 yields three bands (uncleaved protein and two cleavage products), which is consistent with previous results (Ishihara et al., 2006). The longer cleavage product reflects

a cleavage site (S1) in exon 5, and the shorter product reflects a cleavage site (S2) in exon 5b. The deletion of S1 abolishes the longer cleavage product, and it causes an accumulation of uncleaved protein. This uncleaved protein is poorly cleaved upon treatment with CCCP, suggesting that the S2 site is less efficiently cleaved by the inducible protease. Similar results were obtained with Yme1 siRNA. The uncleaved protein that accumulates with Yme1 siRNA is preferentially cleaved at S1 upon induction with CCCP (Fig. 2 D, bottom; lanes 5 and 6).

To confirm that exon 4b– and 5b-containing isoforms are affected by Yme1, we transfected cells with siRNA oligonucleotides that are specific for exons 4b and 5b as described previously (Olichon et al., 2007). Exon 4b and 5b siRNA both reduce the intensity of band d (Fig. S2 A, available at http://www.jcb.org/cgi/content/full/jcb.200704112/DC1). Exon 5b siRNA also reduces the intensity of bands a and c, although these are already faint in wild-type cells. Transfection with Yme1 siRNA produces a pattern that appears to be the sum of exon 4b and 5b siRNA alone. We conclude that the shorter products in uninduced cells consist of isoforms with exon 4b or 5b. These isoforms require Yme1 for constitutive cleavage, whereas the other isoforms remain susceptible to inducible cleavage.

Effects of Yme1 and Opa1 isoform-specific siRNA on mitochondrial morphology

To our surprise, the mitochondria of cells transfected with Yme1 siRNA are unusually connected (Fig. 3, C and D). 2 d after transfection, 40% of cells had more connected mitochondria, 56% appeared normal, and 4% had fragmented mitochondria ($n = 400$), whereas in untransfected cells, 100% of the mitochondria had normal morphologies ($n = 100$). Similar morphological defects were observed with two other Yme1 siRNA oligonucleotides (Fig. S2, B–D), confirming that these effects were specific for the knockdown of Yme1. The increased connectivity is strikingly similar to the connectivity observed with Drp1 siRNA (Fig. 3 B). At later times, a substantial fraction of cells undergo cell death (Fig. S2 E), and the mitochondria fragment (3 d after transfection, 23% of cells had connected mitochondria and 45% were normal, whereas 31% had fragmented mitochondria; $n = 300$). These fragments are more irregular than the mitochondrial fragments in Opa1 siRNA cells (Fig. 3, E and F). Similar mitochondrial disintegration is observed with strong Drp1 mutants at later time points (Smirnova et al., 2001).

To determine whether the increased connectivity of Yme1 siRNA cells is caused by an increase in fusion or a decrease in division, we induced mitochondrial fragmentation by incubating transfected cells with CCCP and allowing them to recover (similar to the cycloheximide experiment; Fig. S1). We find that transfection with Yme1 siRNA does not prevent CCCP-induced fragmentation nor does it prevent recovery after washout (Fig. 4, A–F). Quantitation of these results suggests that there is some delay in recovery (Fig. 4 G), but the fact that recovery can occur at all suggests that Yme1 is not necessary for mitochondrial fusion. The observation that CCCP can still induce mitochondrial fragmentation in Yme1 siRNA cells unlike cells transfected with dominant-negative mutants of Drp1 (Duvezin-Caubet et al., 2006) suggests that mitochondrial fission can still occur as well.
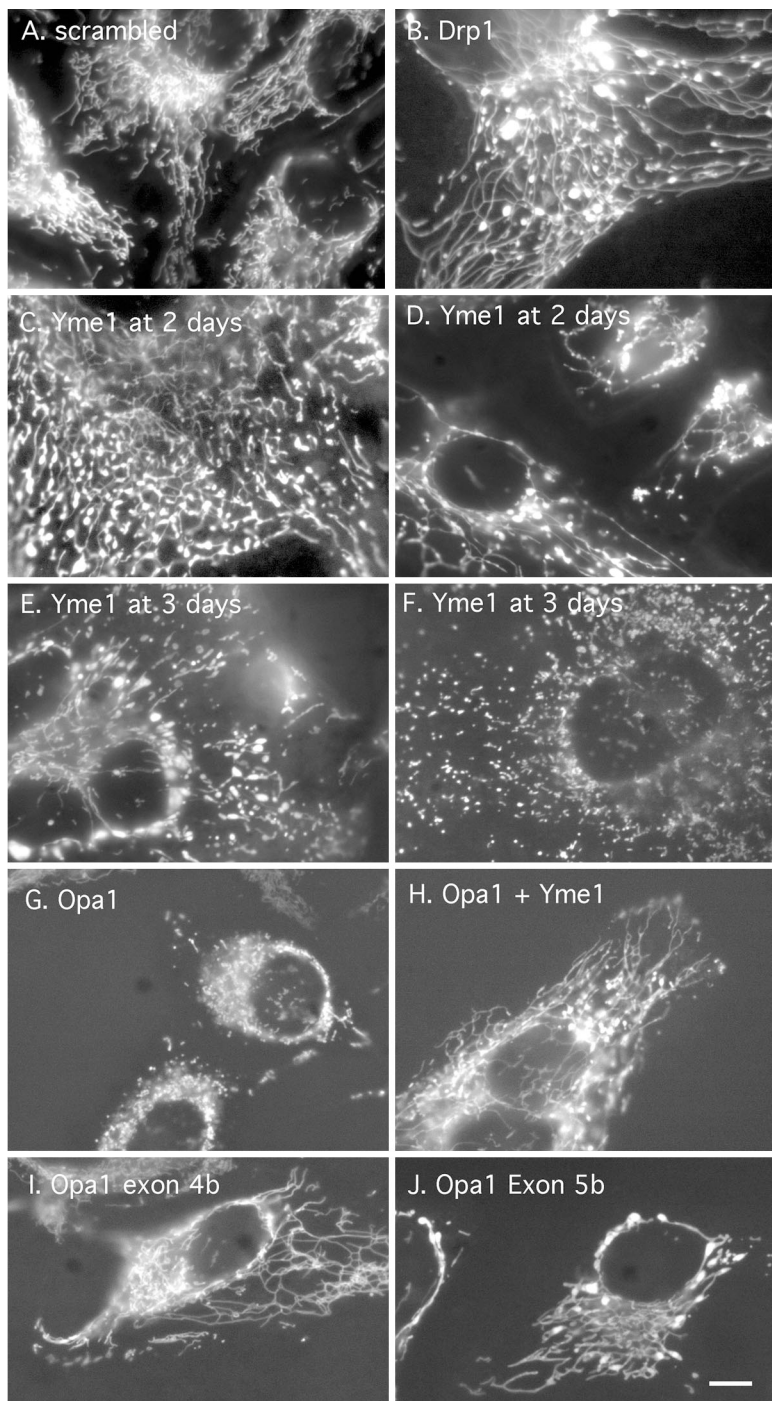
Figure 3. **Disruption of mitochondrial morphology by Yme1 siRNA.** Mitochondria were detected with Mitotracker. (A) Cells transfected with scrambled oligonucleotides for Yme1. (B) A cell 2 d after transfection with Drp1 siRNA. (C and D) Cells 2 d after transfection with Yme1 siRNA. (E and F) Cells 3 d after transfection with Yme1 siRNA. (G) Cells 2 d after transfection with Opa1 siRNA. (H) Cells 2 d after cotransfection with Opa1 and Yme1 siRNA (see Fig. S3 A for expression levels). (I and J) Cells transfected with Opa1 exon 4b– and 5b-specific siRNA (see Fig. S2 for quantification of the morphological defects; available at http://www.jcb.org/cgi/content/full/jcb.200704112/DC1). Bar, 10 μm.

The morphological abnormalities that we observe in Yme1 siRNA cells must therefore result from a subtle shift in the balance between mitochondrial fission and fusion rather than from strong effects on either process.

Comparable morphological abnormalities were also observed with Opa1 exon 4b– and 5b-specific siRNA (Olichon et al., 2007). Transfection with these oligonucleotides increases mitochondrial connectivity (Fig. 3, I and J), but there are small differences between the morphologies observed with exon 4b and 5b siRNA. Exon 4b siRNA gives rise to thin and more connected mitochondria, whereas exon 5b gives rise to connected

mitochondria with localized swellings, similar to Yme1 siRNA. In addition, Opa1 exon 4b– and 5b-specific siRNA increase the number of apoptotic cells (unpublished data), which is consistent with previously published data (Olichon et al., 2007). To determine whether Opa1 is required for the increased connectivity observed with Yme1 siRNA, we cotransfected Yme1 siRNA and pan-Opa1 siRNA. Western blotting showed an 82% reduction of Opa1 levels, which would ordinarily affect mitochondrial morphology (Cipolat et al., 2004), and a 99% reduction of Yme1 levels (see Fig. S3 A for Western blots; available at http://www.jcb.org/cgi/content/full/jcb.200704112/DC1).

Figure 4. **Recovery of Yme1 siRNA–transfected cells from CCCP-induced mitochondrial fragmentation.** (A–F) Cells were transfected with scrambled (A–C) or Yme1 siRNA oligonucleotides (D–F). Mitochondrial morphology was observed by cotransfection with mitochondrial targeted DsRed. Cells was observed without further treatment at 2 d after transfection (A and D), after incubation with CCCP for 60 min (B and E), or incubation with CCCP for 60 min followed by washout and 3.5-h recovery (C and F). (G) Percentages of cells with different mitochondrial morphologies and the treatments described in A–F. Morphologies were classified as connected (highly interconnected), normal (tubular morphology), intermediate (partially fragmented), and fragmented (fully fragmented). Samples sizes for the scrambled controls were as follows: $n = 506$ cells counted before the addition of CCCP, $n = 246$ counted after adding CCCP, and $n = 100$ cells counted at 3.5 h after washout. Sample sizes for Yme1 siRNA were $n = 384$, $n = 332$, and $n = 169$, respectively. Bar, 10 μm.
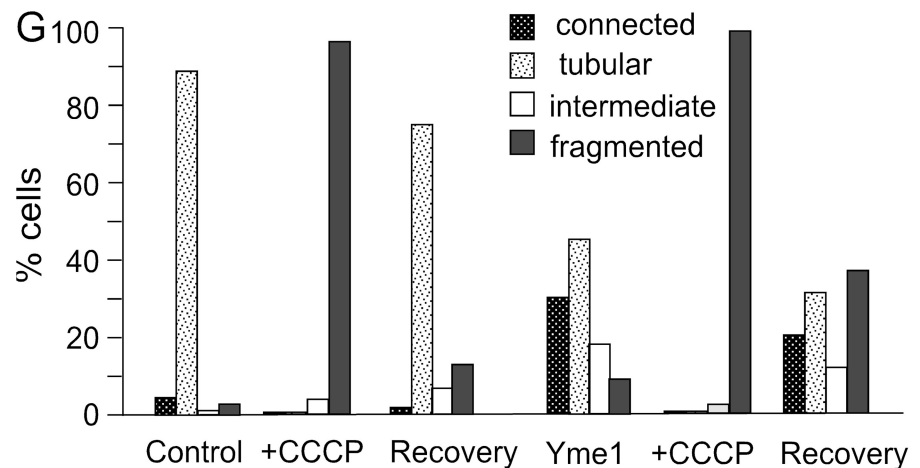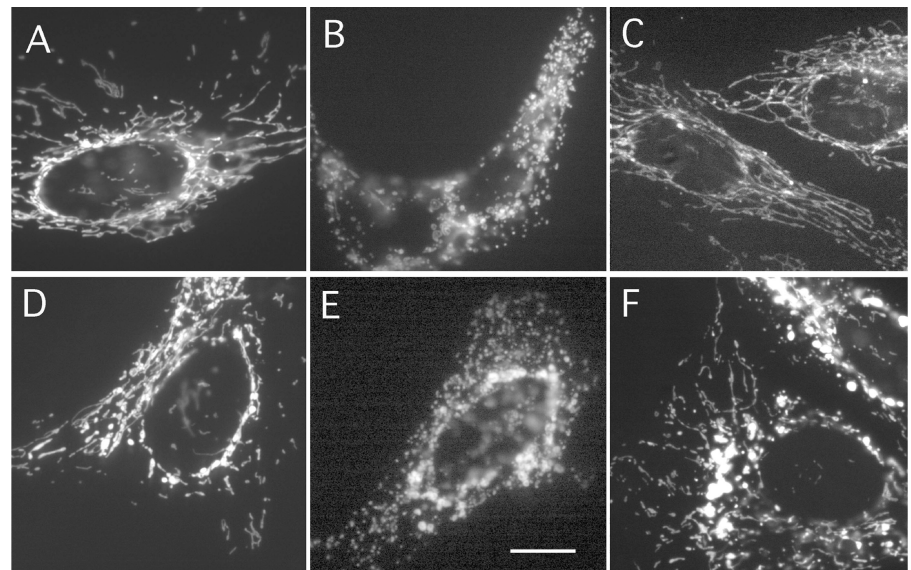
To our surprise, almost all of the cells that were cotransfected with Opa1 and Yme1 siRNA had more connected mitochondria (Fig. 3 H), similar to Yme1 siRNA alone, whereas none had fragmented mitochondria ($n = 200$). In contrast, 99% of cells that were transfected with Opa1 siRNA alone had fragmented mitochondria, as seen previously (Griparic et al., 2004). These results suggest that Yme1 is epistatic to Opa1.

We used electron microscopy to examine the effects of Yme1 siRNA on the internal structure of mitochondria (Fig. S3, C–F). For comparison, cells were also transfected with Drp1 siRNA and with Yme1 and Opa1 siRNA together. None of these transfections had drastic effects on cristae morphology. Yme1 siRNA did cause some cristae to appear disorganized, but the results were not strong nor were they readily quantified. There were also no obvious defects in Yme1/Opa1 double siRNA cells. Opa1 siRNA can affect cristae morphology (Griparic et al., 2004), but this might have been suppressed by the increased connectivity caused by Yme1 siRNA. Similar suppression of cristae defects was observed in a yeast double mutant of Mgm1 and Dnm1 (homologues of Opa1 and Drp1; Sesaki et al., 2003). We conclude that the internal structures of mitochondria are not notably disrupted by Yme1 siRNA.

Functional consequences of Opa1 proteolysis

Our results show a distinction between the constitutive cleavage of Opa1, which is Yme1 dependent, and inducible cleavage, which is Yme1 independent. These two types of cleavage have different effects on different isoforms. The processing of isoforms 5 (exon 4b) and 7 (exon 5b) requires Yme1, whereas isoform 1 (neither exon) is unaffected by Yme1. Yme1 renders isoforms with exons 4b and 5b insensitive to inducible cleavage, whereas the loss of Yme1 with siRNA restores their sensitivity to inducible cleavage. Yme1 could directly cleave Opa1 because both proteins are anchored in the mitochondrial inner membrane facing the mitochondrial inner membrane space, or the effects could be indirect. Based on these results, we propose that the Opa1 isoforms fall into two classes: namely, those that are sensitive to Yme1 and those that are not.

Although better known for its role in the proteolytic degradation of misfolded proteins (Langer et al., 2001), Yme1 has been shown to assist the import and maturation of specific intermembrane space proteins (Rainey et al., 2006). However, cells transfected with Yme1 siRNA or with exon 4b or 5b siRNA do not show an obvious fusion defect. Instead, these transfections

lead to novel mitochondrial morphologies that are more similar to the morphologies in preapoptotic cells, which is consistent with the previously proposed antiapoptotic function of exons 4b and 5b (Olichon et al., 2007).

It is not yet clear how Yme1 siRNA affects mitochondrial morphology. Yme1 could directly influence mitochondrial fission or fusion, or it could act on a different protein with a dominant effect on mitochondrial morphology. However, increased numbers of connections were also observed in *Drosophila melanogaster* cells treated with ceramide, suggesting that this might be a prelude to apoptosis (Goyal et al., 2007). Yme1 siRNA might then preempt the loss of fusion caused by Opa1 siRNA in cotransfected cells by increasing the rate of mitochondrial fusion or decreasing the rate of fission at an earlier time point. These effects are not absolute, however, because they are overridden by treatment with CCCP. A similar dichotomy was observed with BH3 proteins such as Bax and Bak, which direct mitochondrial fission during apoptosis but are required for mitochondrial fusion in normal cells (Karbowski et al., 2006).

The accompanying paper by Song et al. (see p. 749 of this issue) and previous work with yeast (Herlan et al., 2003) show that mitochondrial fusion requires both cleaved and uncleaved forms of Opa1. Song et al. (2007) show that Yme1 can mediate this cleavage, but our data indicate that fusion also occurs without Yme1. The requirement for cleavage, which is shown by Song et al. (2007), might instead be met by the inducible protease. This possibility is intriguing because the inducible protease and mitochondrial fusion are both regulated by the mitochondrial inner membrane potential (Meeusen et al., 2004). We conclude that there are three types of Opa1 cleavage: (1) Yme1-dependent processing of Opa1 isoforms with antiapoptotic functions; (2) cleavage of a fraction of Opa1 protein to meet the requirement for fusion; this type of cleavage can be mediated by Yme1, but it might also be mediated by the inducible protease; and (3) inducible cleavage of the remaining Opa1 protein after the loss of membrane potential as it occurs during apoptosis. This cleavage probably inactivates Opa1 because it coincides with mitochondrial fragmentation.

Materials and methods

Cell culture and microscopy
HeLa cells were cultured as described previously (Griparic et al., 2004). Apoptosis was induced with 2 μM staurosporine (Sigma-Aldrich) or 10 μM actinomycin D (Calbiochem). Where indicated, 100 μM zVAD-fmk (Qbiogene) was added 30 min before adding actinomycin D. Mitochondrial membrane potential was disrupted with 10 μM CCCP (Sigma-Aldrich), and, where indicated, 20 μg/ml cycloheximide (Calbiochem) was added. For the washout experiments, cells were rinsed twice with PBS at 37°C and incubated with fresh culture medium. Controls were treated with solvent (DMSO). Cells were prepared for immunofluorescence as described previously (Griparic et al., 2004). Opa1 antibody was described previously (Griparic et al., 2004). Apoptosis-inducing factor antibody was obtained from Santa Cruz Biotechnology, Inc., and cytochrome *c* antibody was purchased from BD Biosciences. Secondary antibodies were purchased from Jackson ImmunoResearch Laboratories and Biomeda. B. De Strooper (Katholieke Universiteit Leuven, Leuven, Belgium) provided PARL knockout mouse embryonic fibroblast cells, which were grown as described previously (Cipolat et al., 2006). Fluorescence microscopy was performed with a microscope (Axiovert 200M; Carl Zeiss MicroImaging, Inc.) using an α plan-Fluar 100× NA 1.45 oil objective (Carl Zeiss MicroImaging, Inc.). Images were acquired with a CCD camera (ORCA ER; Hamamatsu) and

Axiovision software (Carl Zeiss MicroImaging, Inc.). Image files were processed with Photoshop software (Adobe).

Subcellular fractionation and Western blotting
To isolate mitochondria for the Yme1 blots, cells were pelleted by centrifugation for 5 min at 600 *g* and washed with mitochondrial isolation buffer (Griparic et al., 2004). Cell membranes were disrupted by sonication. Nuclei and unbroken cells were removed by centrifugation for 5 min at 1,000 *g*. Mitochondria were pelleted by further centrifugation for 30 min at 10,000 *g*. Pellets were resuspended in laemmli sample buffer, size fractionated by SDS-PAGE, and blotted to nitrocellulose.

Cell extracts were produced by direct lysis in laemmli sample buffer. After boiling for 5 min, samples were resolved by SDS-PAGE (6% for Opa1 and 10 or 12% for the other proteins). Blots were probed with mouse Opa1 and Tim23 antibodies (BD Biosciences), mouse caspase 9 and PARP antibodies (BD Biosciences), caspase 3 antibody (Abcam), Omi antibody (BioVision), rat anti-myc antibody (AbD Serotec), goat anti-Hsp60 antibody (Santa Cruz Biotechnology, Inc.), and tubulin monoclonal antibody (Sigma-Aldrich). PARL antibodies were provided by B. De Strooper, and Yme1 antibodies were provided by C. Koehler (University of California, Los Angeles, Los Angeles, CA). Blots were developed with HRP-labeled secondary antibody and chemiluminescence reagents (GE Healthcare).

Transfection constructs and siRNA oligonucleotides
The expression construct containing wild-type Opa1 isoform 1 was described previously (Griparic et al., 2004). A C-terminal myc tag was added to this construct by PCR. Isoform 7 was generated by amplifying exon 5b from HeLa cDNA and cloning this fragment with BclI and BstBI sites in the myc-tagged isoform 1 construct. Isoform 5 was similarly generated by amplifying exon 4b and surrounding sequences from HeLa cDNA and cloning this fragment with BclI and BstBI sites in the myc-tagged isoform 1 construct. Deletions in the S1 cleavage site were made with fusion PCR using AGGTTCTCCGGAAGAATCTGAAAGTGACAAGCATTTTAG and AATGCTTGTCACTTTCAGATTCTTCCGGAGAACCTGAGGT primers for site-directed mutagenesis. The mutated fragments were cloned into the isoform 1, 5, and 7 myc-tagged constructs with BclI and BstBI sites. New clones were sequenced to ensure fidelity.

The oligonucleotides for siRNA were synthesized by Sigma-Proligo. Their sequences are GATGCATTTAAAACTGGTTTT (first), ACTTCCAAAAGG-AATTCTTTT (second), and TCTTGTGAACCAGGCTGCATT (third) for Yme1, ATCCAGGGTCCAGAGTTATTT for PARL, GGTCACAGCTGGAATCTCCTT for HtrA2/Omi, GGGAAGGTGGATTCAGTGCTT and TCAGCTTAAAATG-GCTCGTTT for paraplegin, TATTGGCAGTGTGGACACCTT and GAATGCC-CCTTGCATCCTCTT for AFG3L2, GCAGAAGAATGGGGTAAATTT for Drp1, GATCATCTGCCACGGGTTGTT for all Opa1 isoforms, GTCATAGGAGCTT-CTGACCTA for Opa1 exon 4b, and GAGGAAGCGCGCAGAGCCGCT for Opa1 exon 5b of Opa1. Scrambled controls had inverted sense strand sequences. HeLa cells were split 1 d before transfection, giving 30–50% confluency on the next day. Transfection was performed with Oligofectamine (Invitrogen) using 60 pmol siRNA duplexes. On day 2, cells were split 1:3 or 1:4 to 6-cm or glass-bottom dishes and transfected again on day 3. On day 4, some cells were used for RNA isolation. Others were incubated with Mito-Tracker red (Invitrogen) and CCCP. For CCCP recovery with Yme1 siRNA, cells were transfected with siRNA and MitoDsRed (CLONTECH Laboratories, Inc.) using LipofectAMINE 2000 (Invitrogen).

The effects of siRNA on expression levels were quantified with real-time PCR or with Western blotting when antibodies were available. For real-time PCR, total RNA was isolated with the RNeasy kit (QIAGEN). 200–300 ng RNA was reverse transcribed using ThermoScript (Invitrogen). Real-time PCR was performed with an ICycler and iQ SYBR green Supermix (Bio-Rad Laboratories). Actin mRNA was used as a control. Each sample was measured in triplicate. Western blots were quantified with densitometry using a Personal Densitometer SI and ImageQuant software (Molecular Dynamics).

Online supplemental material
Fig. S1 shows the CCCP-induced cleavage of Opa1 and recovery after washout (A) and that mitochondria also recover their filamentous morphology, but not with cycloheximide (B–E). Fig. S2 shows the effects of Yme1 siRNA on Opa1 and compares this with the effects of exon 4b and 5b siRNA (A). Fig. S2 also shows the morphological effects of two additional Yme1 siRNA oligonucleotides (B–D) and shows the effects of Yme1 siRNA on apoptosis (E). Fig. S3 shows Opa1 and Yme1 in single and double siRNA transfections by Western blotting and electron microscopy. Table S1 presents data on the percentage of cells releasing Opa1, cytochrome *c*, or apoptosis-inducing factor from mitochondria 7 or 10 h after inducing

References

Arnoult, D., A. Grodet, Y.J. Lee, J. Estaquier, and C. Blackstone. 2005. Release of OPA1 during apoptosis participates in the rapid and complete release of cytochrome c and subsequent mitochondrial fragmentation. *J. Biol. Chem.* 280:35742–35750.

Cipolat, S., O. Martins de Brito, B. Dal Zilio, and L. Scorrano. 2004. OPA1 requires mitofusin 1 to promote mitochondrial fusion. *Proc. Natl. Acad. Sci. USA.* 101:15927–15932.

Cipolat, S., T. Rudka, D. Hartmann, V. Costa, L. Serneels, K. Craessaerts, K. Metzger, C. Frezza, W. Annaert, L. D'Adamio, et al. 2006. Mitochondrial rhomboid PARL regulates cytochrome c release during apoptosis via OPA1-dependent cristae remodeling. *Cell.* 126:163–175.

Duvezin-Caubet, S., R. Jagasia, J. Wagener, S. Hofmann, A. Trifunovic, A. Hansson, A. Chomyn, M.F. Bauer, G. Attardi, N.G. Larsson, et al. 2006. Proteolytic processing of OPA1 links mitochondrial dysfunction to alterations in mitochondrial morphology. *J. Biol. Chem.* 281:37972–37979.

Frezza, C., S. Cipolat, O. Martins de Brito, M. Micaroni, G.V. Beznoussenko, T. Rudka, D. Bartoli, R.S. Polishuck, N.N. Danial, B. De Strooper, and L. Scorrano. 2006. OPA1 controls apoptotic cristae remodeling independently from mitochondrial fusion. *Cell.* 126:177–189.

Goyal, G., B. Fell, A. Sarin, R.J. Youle, and V. Sriram. 2007. Role of mitochondrial remodeling in programmed cell death in *Drosophila melanogaster*. *Dev. Cell.* 12:807–816.

Griparic, L., N.N. van der Wel, I.J. Orozco, P.J. Peters, and A.M. van der Bliek. 2004. Loss of the intermembrane space protein Mgm1/OPA1 induces swelling and localized constrictions along the lengths of mitochondria. *J. Biol. Chem.* 279:18792–18798.

Herlan, M., F. Vogel, C. Bornhövd, W. Neupert, and A.S. Reichert. 2003. Processing of Mgm1 by the Rhomboid -type protease Pcp1 is required for maintenance of mitochondrial morphology and of mitochondrial DNA. *J. Biol. Chem.* 278:27781–27788.

Ishihara, N., Y. Fujita, T. Oka, and K. Mihara. 2006. Regulation of mitochondrial morphology through proteolytic cleavage of OPA1. *EMBO J.* 25:2966–2977.

Karbowski, M., K.L. Norris, M.M. Cleland, S.Y. Jeong, and R.J. Youle. 2006. Role of Bax and Bak in mitochondrial morphogenesis. *Nature.* 443:658–662.

Langer, T., M. Kaser, C. Klanner, and K. Leonhard. 2001. AAA proteases of mitochondria: quality control of membrane proteins and regulatory functions during mitochondrial biogenesis. *Biochem. Soc. Trans.* 29:431–436.

McQuibban, G.A., S. Saurya, and M. Freeman. 2003. Mitochondrial membrane remodelling regulated by a conserved rhomboid protease. *Nature.* 423:537–541.

Meeusen, S.L., and J. Nunnari. 2005. How mitochondria fuse. *Curr. Opin. Cell Biol.* 17:389–394.

Meeusen, S., J.M. McCaffery, and J. Nunnari. 2004. Mitochondrial fusion intermediates revealed in vitro. *Science.* 305:1747–1752.

Meeusen, S., R. DeVay, J. Block, A. Cassidy-Stone, S. Wayson, J.M. McCaffery, and J. Nunnari. 2006. Mitochondrial inner-membrane fusion and crista maintenance requires the dynamin-related GTPase Mgm1. *Cell.* 127:383–395.

Olichon, A., L. Baricault, N. Gas, E. Guillou, A. Valette, P. Belenguer, and G. Lenaers. 2003. Loss of OPA1 perturbates the mitochondrial inner membrane structure and integrity, leading to cytochrome c release and apoptosis. *J. Biol. Chem.* 278:7743–7746.

Olichon, A., G. Elachouri, L. Baricault, C. Delettre, P. Belenguer, and G. Lenaers. 2007. OPA1 alternate splicing uncouples an evolutionary conserved function in mitochondrial fusion from a vertebrate restricted function in apoptosis. *Cell Death Differ.* 14:682–692.

Rainey, R.N., J.D. Glavin, H.W. Chen, S.W. French, M.A. Teitell, and C.M. Koehler. 2006. A new function in translocation for the mitochondrial i-AAA protease Yme1: import of polynucleotide phosphorylase into the intermembrane space. *Mol. Cell. Biol.* 26:8488–8497.

Satoh, M., T. Hamamoto, N. Seo, Y. Kagawa, and H. Endo. 2003. Differential sublocalization of the dynamin-related protein OPA1 isoforms in mitochondria. *Biochem. Biophys. Res. Commun.* 300:482–493.

Seong, Y.M., J.Y. Choi, H.J. Park, K.J. Kim, S.G. Ahn, G.H. Seong, I.K. Kim, S. Kang, and H. Rhim. 2004. Autocatalytic processing of HtrA2/Omi is essential for induction of caspase-dependent cell death through antagonizing XIAP. *J. Biol. Chem.* 279:37588–37596.

Sesaki, H., S.M. Southard, M.P. Yaffe, and R.E. Jensen. 2003. Mgm1p, a dynamin-related GTPase, is essential for fusion of the mitochondrial outer membrane. *Mol. Biol. Cell.* 14:2342–2356.

Smirnova, E., L. Griparic, D.L. Shurland, and A.M. van der Bliek. 2001. Dynamin-related protein Drp1 is required for mitochondrial division in mammalian cells. *Mol. Biol. Cell.* 12:2245–2256.

Song, Z., H. Chen, M. Fiket, C. Alexander, and D.C. Chan. 2007. OPA1 processing controls mitochondrial fusion and is regulated by mRNA splicing, membrane potential, and Yme1L. *J. Cell Biol.* 178: 749–755.

van der Bliek, A.M. 1999. Functional diversity in the dynamin family. *Trends Cell Biol.* 9:96–102.

van der Bliek, A.M., and C.M. Koehler. 2003. A mitochondrial rhomboid protease. *Dev. Cell.* 4:769–770.

Votruba, M. 2004. Molecular genetic basis of primary inherited optic neuropathies. *Eye.* 18:1126–1132.

Wong, E.D., J.A. Wagner, S.V. Scott, V. Okreglak, T.J. Holewinske, A. Cassidy-Stone, and J. Nunnari. 2003. The intramitochondrial dynamin-related GTPase, Mgm1p, is a component of a protein complex that mediates mitochondrial fusion. *J. Cell Biol.* 160:303–311.